

Fixed versus adaptive irrigation and fertilizer management under weather uncertainty: a comparative study using genetic algorithm optimization and model predictive control

Carla J. Becker^{1*} and Tarek I. Zohdi¹

¹*Department of Mechanical Engineering, University of California, Berkeley, 6141 Etcheverry Hall, Berkeley, 94720, California, United States of America.

*Corresponding author(s). E-mail(s): carlabecker@berkeley.edu, ORCID: [0009-0004-0646-6386](https://orcid.org/0009-0004-0646-6386);

Contributing authors: zohdi@berkeley.edu, ORCID: [0000-0002-0844-3573](https://orcid.org/0000-0002-0844-3573);

Abstract

Climate variability poses significant challenges to agricultural resource management, as fixed irrigation and fertilization strategies optimized for expected conditions may perform poorly when actual weather deviates from assumptions. This paper presents a comparative study of fixed versus adaptive resource management strategies under weather uncertainty. We develop an adaptive approach combining Model Predictive Control (MPC) with Bayesian Optimization (BO) for irrigation and fertilizer scheduling, building on a crop growth model that captures delayed nutrient absorption via finite impulse response (FIR) convolution and cumulative stress tracking via exponential moving average (EMA) filtering. The MPC controller solves a constrained finite-time optimal control (CFTOC) problem at each decision epoch, balancing crop value maximization against input costs and nutrient stress penalties, with BO using Tree-structured Parzen Estimators (TPE) to tune controller parameters for robust performance. Evaluated on corn production in Iowa across 21 stochastic weather scenarios ranging from normal to extreme conditions, we compare three strategies: farmer baseline practices, a genetic algorithm (GA) that optimizes a fixed strategy for drought conditions, and adaptive MPC that re-optimizes daily. Results reveal a fundamental tradeoff between mean revenue and consistency. The fixed GA achieves the highest mean revenue (\$796/acre) but with substantial variance, while MPC achieves lower mean revenue (\$750/acre) but with the lowest coefficient of variation (15.4% vs 16.6%). MPC outperforms GA in 12 of 21 scenarios—particularly in normal and wet conditions—while GA excels in the drought conditions for which it was optimized. These findings provide practical guidance: when weather patterns are predictable and match optimization assumptions, fixed strategies maximize returns; when weather is uncertain, adaptive MPC provides valuable risk reduction through consistent performance across diverse conditions.

Keywords: precision agriculture, model predictive control, Bayesian optimization, weather uncertainty, adaptive control

1 Introduction

Climate change is increasing the frequency and severity of extreme weather events, posing significant challenges to agricultural production [1]. Traditional approaches to irrigation and fertilizer scheduling rely on fixed strategies—either following agronomic best practices or optimized once for expected conditions—that cannot adapt when actual weather deviates from assumptions. As drought, heat waves, and other extremes become more common, there is growing need for adaptive resource management strategies that can respond to observed conditions in real time. Recent work on digital-twin frameworks for precision

agriculture [2, 3] and computational approaches to agricultural resource delivery [4, 5] has demonstrated the potential for model-based optimization in farming systems.

In a companion paper currently under review [6], we developed a generalized crop growth model based on coupled ordinary differential equations (ODEs) that captures the nonlinear dynamics of plant development under varying environmental conditions. The model tracks five state variables—plant height, leaf area, number of leaves, flower size, and fruit biomass—each governed by logistic growth with time-varying parameters modulated by nutrient factors. These factors quantify how well actual water, fertilizer, temperature, and solar radiation levels match the plant’s physiological expectations, with delayed absorption modeled via finite impulse response (FIR) convolution and cumulative stress tracked via exponential moving average (EMA) filtering. Using a genetic algorithm (GA), we showed that optimized irrigation and fertilizer strategies can achieve 16% higher net revenue than conventional farmer practices under drought conditions.

However, the GA approach optimizes a *fixed* strategy—specifying application frequencies and amounts that remain constant throughout the growing season. While effective when actual conditions match the optimization assumptions, such open-loop strategies cannot adapt to unexpected weather events. If a drought is more severe than anticipated, or an unexpected heat wave occurs, the pre-computed strategy may be far from optimal.

This paper extends our previous work by developing an *adaptive* approach using Model Predictive Control (MPC). MPC is a closed-loop control strategy that repeatedly solves an optimization problem over a finite horizon, applies only the first control action, then re-optimizes based on updated state and disturbance information [7]. This receding-horizon structure enables the controller to adapt to changing conditions while maintaining optimality over the planning horizon.

Applying MPC to agricultural systems presents several challenges. First, the nonlinear crop dynamics with delayed absorption effects complicate the optimization problem. Second, the controller must balance multiple competing objectives: maximizing crop value, minimizing input costs, and avoiding nutrient stress that degrades plant health. Third, the relative importance of these objectives depends on weather conditions and growth stage, requiring careful tuning of the cost function weights. To address this last challenge, we employ Bayesian Optimization (BO) [8] to automatically tune the MPC parameters for robust performance across diverse weather scenarios.

Our contributions are:

1. Formulation of a constrained finite-time optimal control (CFTOC) problem for daily irrigation and fertilizer scheduling that accounts for delayed nutrient absorption and cumulative stress effects.
2. A receding-horizon MPC implementation that adapts resource allocation based on observed weather conditions, with parameters tuned via Bayesian optimization using Tree-structured Parzen Estimators (TPE) [9].
3. Systematic comparison of three resource management strategies—farmer baseline, fixed GA-optimized, and adaptive MPC—across 21 stochastic weather scenarios spanning normal to extreme conditions.
4. Characterization of the risk-return tradeoff between fixed and adaptive strategies, identifying the conditions under which each approach excels.

Our results reveal that the choice between fixed and adaptive strategies involves a fundamental tradeoff. The GA-optimized fixed strategy achieves higher mean revenue but with greater variance, while MPC sacrifices some peak performance for consistency across diverse weather conditions. These findings provide practical guidance for agricultural decision-making under climate uncertainty.

2 Crop growth model

We employ the crop growth model developed in [6], which we briefly summarize here. The model treats the plant as a dynamic system with state vector $x = [x_h, x_A, x_N, x_c, x_P]^T$ representing plant height (m), leaf area per leaf (m^2), number of leaves, flower size (spikelets), and fruit biomass (kg). Control inputs are irrigation u_w (inches/hour) and fertilizer u_f (lbs/hour), while disturbances include precipitation d_S (inches/hour), temperature d_T ($^\circ\text{C}$), and solar radiation d_R (W/m^2).

2.1 Logistic growth dynamics

Each state variable follows logistic growth with time-varying parameters:

$$\frac{dx}{dt} = \hat{a}_x(t) \cdot x(t) \left(1 - \frac{x(t)}{\hat{k}_x(t)}\right) \quad (1)$$

where $\hat{a}_x(t)$ is the effective growth rate and $\hat{k}_x(t)$ is the effective carrying capacity, both modulated by nutrient factors. This equation admits a closed-form solution:

$$x(t + \Delta t) = \frac{\hat{k}_x(t)}{1 + \left(\frac{\hat{k}_x(t)}{x(t)} - 1\right) \exp(-\hat{a}_x(t)\Delta t)} \quad (2)$$

enabling exact time-stepping without numerical integration error.

2.2 Delayed absorption via FIR convolution

Plants do not immediately utilize applied nutrients; there is a physiologically-mediated delay between application and absorption. We model this using finite impulse response (FIR) convolution with Gaussian kernels:

$$g[k] = \frac{1}{\sqrt{2\pi\sigma^2}} \exp\left\{-\frac{(k-\mu)^2}{2\sigma^2}\right\} \quad (3)$$

where σ is the temporal spread characterizing absorption duration. We set $\mu \approx 1.96\sigma$ so that 95% of the kernel mass lies within $[0, 2\mu]$. Different nutrients have different metabolic timescales: $\sigma_w = 30$ hours for water (rapid uptake), $\sigma_f = 300$ hours for fertilizer (slow root absorption), and $\sigma_T = \sigma_R = 30$ hours for temperature and radiation.

The delayed (absorbed) signal is computed as:

$$\bar{u}[k] = \sum_{n=0}^{L-1} g[n] \cdot u[k-n] \quad (4)$$

where L is the FIR horizon chosen to capture 95% of the kernel mass.

2.3 Cumulative stress tracking

While FIR convolution captures delayed absorption, plants also accumulate stress from sustained deviations from optimal conditions. We track cumulative divergence using exponential moving average (EMA) filtering:

$$\Delta_u[k] = \beta_\Delta \cdot \Delta_u[k-1] + (1 - \beta_\Delta) \cdot \delta_u[k] \quad (5)$$

where $\delta_u[k]$ is the instantaneous anomaly (relative deviation from expected cumulative absorption) and $\beta_\Delta = 0.95$ provides long memory of past stress events.

2.4 Nutrient factors

The cumulative divergence is converted to a nutrient factor $\nu \in [0, 1]$ via exponential decay with additional EMA smoothing:

$$\nu_u[k] = \beta_\nu \cdot \nu_u[k-1] + (1 - \beta_\nu) \cdot \exp\{-\alpha\Delta_u[k]\} \quad (6)$$

where $\alpha = 3$ ensures $\nu \approx 0.05$ when $\Delta = 1$ (complete divergence). The nutrient factor equals 1 when inputs match expectations and decays toward 0 under sustained stress.

The effective growth parameters are computed as geometric means of relevant nutrient factors. For example, fruit biomass carrying capacity depends on all inputs and prior vegetative growth:

$$\hat{k}_P(t) = k_P \left(\nu_w \nu_f \nu_T \nu_R \frac{\hat{k}_h}{k_h} \frac{\hat{k}_A}{k_A} \frac{\hat{k}_c}{k_c} \right)^{1/7} \quad (7)$$

Full details of the parameter relationships are provided in [6].

3 Stochastic weather scenario generation

To evaluate controller robustness, we generate a suite of stochastic weather scenarios from historical baseline data. Each scenario applies perturbations representing different climate conditions, from normal variability to extreme events.

3.1 Generation process

Let the historical hourly time series be

$$d_S^{\text{hist}}[k] \geq 0 \quad (8)$$

$$-20 \leq d_T^{\text{hist}}[k] \leq 50 \quad (9)$$

$$d_R^{\text{hist}}[k] \geq 0 \quad (10)$$

for $k = 0, \dots, K - 1$ where K is the length of the growing season in hours, respectively representing precipitation (inches), temperature ($^{\circ}\text{C}$), and solar radiation (W/m^2). Then, let a stochastic weather scenario be defined by the parameters

$$\theta = (s_S, s_T, s_R, \eta, \mathcal{D}, \mathcal{H}, \mathcal{C}) \quad (11)$$

where

- s_S is the precipitation scaling factor
- s_T is the temperature offset
- s_R is the radiation scaling factor
- η is the relative noise level (a fraction of the historical standard deviation)
- \mathcal{D} is a drought event
- \mathcal{H} is a heat wave event
- \mathcal{C} is a cold snap event

Each of the event types $(\mathcal{D}, \mathcal{H}, \mathcal{C})$ are defined by three parameters:

$$[k_0, \kappa, \iota] \quad (12)$$

where

- k_0 is the hour when the event begins
- κ is the duration of the event in number of hours
- $\iota \in [0, 1]$ is the intensity, with 1 being the most intense

3.1.1 Global scaling and offset

Initialize the synthetic environmental disturbance time series after applying the global adjustments (s_S, s_T, s_R) for $k = 0, \dots, K - 1$ as below

$$\begin{aligned} d_S^{(1)}[k] &= s_S d_S^{\text{hist}}[k] && \text{(scaling)} \\ d_T^{(1)}[k] &= d_T^{\text{hist}}[k] + s_T && \text{(offset)} \\ d_R^{(1)}[k] &= s_R d_R^{\text{hist}}[k] && \text{(scaling)} \end{aligned} \quad (13)$$

3.1.2 Add white noise

If $\eta > 0$, draw independent white noise sequences

$$\varepsilon_T[k] \sim \mathcal{N}(0, (\eta \sigma_T)^2) \quad (14)$$

$$\varepsilon_R[k] \sim \mathcal{N}(0, (\eta \sigma_R)^2) \quad (15)$$

where σ_T and σ_R are the standard deviations of the historical temperature and radiation time series, respectively.

We then smooth the white noise with a moving average over $m_T = 24$ hours for temperature and $m_R = 12$ hours for radiation, as we will only apply the noise to the radiation during the day time (when it is not as close to zero).

$$\bar{\varepsilon}_T = \frac{1}{m_T} \sum_{n=0}^{m_T-1} \varepsilon_T[k-n] \quad (16)$$

$$\bar{\varepsilon}_R = \frac{1}{m_R} \sum_{n=0}^{m_R-1} \varepsilon_R[k-n] \quad (17)$$

We then add that noise to the signals:

$$d_T^{(2)}[k] = d_T^{(1)}[k] + \bar{\varepsilon}_T[k] \quad (18)$$

$$d_R^{(2)}[k] = d_R^{(1)}[k] + \mathcal{M}_{\text{day}} \bar{\varepsilon}_R[k] \quad (19)$$

where

$$\mathcal{M}_{\text{day}} = \{k | d_R^{\text{hist}}[k] > d_R^{\text{day}}\} \quad (20)$$

and we choose the threshold $d_R^{\text{day}} = 10 \text{ W/m}^2$. Precipitation is unchanged in this step, so

$$d_S^{(2)}[k] = d_S^{(1)}[k] \quad (21)$$

If $\eta = 0$, then we let $(d_S^{(2)}, d_T^{(2)}, d_R^{(2)}) = (d_S^{(1)}, d_T^{(1)}, d_R^{(1)})$.

3.1.3 Drought injection

A drought event is

$$\mathcal{D} = [k_0, \kappa, \iota] \quad (22)$$

For each event, we define the affected hourly index set as

$$\mathcal{I} = \{k_0, k_0 + 1, \dots, \min(k_0 + \kappa - 1, K - 1)\} \quad (23)$$

and then apply the intensity scaling to those indices with

$$d_S^{(3)}[k] \leftarrow (1 - \iota) d_S^{(2)}[k] \quad \text{for all } k \in \mathcal{I} \quad (24)$$

Temperature and radiation are unchanged in this step, so

$$d_T^{(3)}[k] = d_T^{(2)}[k] \quad \text{and} \quad d_R^{(3)}[k] = d_R^{(2)}[k] \quad (25)$$

3.1.4 Heat wave injection

A heat wave event is

$$\mathcal{H} = [k_0, \kappa, \iota] \quad (26)$$

where k_0 and κ have the same meanings they did for the drought event, but now ι is the peak temperature add (an offset rather than a scaling factor). We then construct a ramp-up, hold, and ramp-down for the heat wave. Let

$$\kappa_{\text{ramp}} = \max(1, 0.1\kappa) \quad (27)$$

i.e. either one tenth of the heat wave duration or at least one hour. Then, let

$$\kappa_{\text{hold}} = \kappa - 2\kappa_{\text{ramp}} \quad (28)$$

to account for the ramp-up and ramp-down.

We can then define

- ramp-up: $w_{\text{up}}[k] = \frac{k}{\kappa_{\text{ramp}} - 1}$ for $k = 0, \dots, \kappa_{\text{ramp}} - 1$
- ramp-up: $w_{\text{hold}}[k] = 1$
- ramp-down: $w_{\text{down}}[k] = \frac{k}{\kappa_{\text{ramp}} - 1}$ for $k = 0, \dots, \kappa_{\text{ramp}} - 1$

and concatenate to form the heat wave window

$$w_{\text{heat}} = [w_{\text{up}}, w_{\text{hold}}, w_{\text{down}}] \quad (29)$$

Applying the heat wave to the temperature time series, we obtain

$$d_T^{(4)}[k] \leftarrow d_T^{(3)}[k] + \iota w_{\text{heat}}[k - k_0] \quad (30)$$

for $k = k_0, k_0 + 1, \dots, \min(k_0 + \kappa - 1, K - 1)$. Precipitation and radiation are unchanged in this step, so

$$d_S^{(4)}[k] = d_S^{(3)}[k] \quad \text{and} \quad d_R^{(4)}[k] = d_R^{(3)}[k] \quad (31)$$

3.1.5 Cold snap injection

A cold snap event is

$$\mathcal{C} = [k_0, \kappa, \iota] \quad (32)$$

where k_0 and κ have the same meanings they did for the heat wave event, but ι is now the magnitude of the lowest temperature drop. A cold snap window is constructed in the same manner as the heat wave window and the temperature time series becomes

$$d_T^{(4)}[k] \leftarrow d_T^{(4)}[k] - \iota w_{\text{heat}}[k - k_0] \quad (33)$$

for $k = k_0, k_0 + 1, \dots, \min(k_0 + \kappa - 1, K - 1)$. Note: we have used $d_T^{(4)}[k]$ on the righthand side because we want to reflect that a heat wave may have already been applied.

3.1.6 Clipping to physical bounds

Finally, we check to ensure that the transformations above have not violated the bounds on the input disturbances specified in equations 10. If they have, we clip the values as below

$$d_S^{\text{syn}}[k] = \max(0, d_S^{(4)}[k]) \quad (34)$$

$$d_T^{\text{syn}}[k] = \min(50, \max(-20, d_T^{(4)}[k])) \quad (35)$$

$$d_R^{\text{syn}}[k] = \max(0, d_R^{(4)}[k]) \quad (36)$$

for all $k \in \{0, \dots, K - 1\}$.

3.2 Extremity index

Extremity from precipitation:

$$\mathcal{E}_{\text{precip}} = 2|1 - s_S| \quad (37)$$

So, $s_S = 1$ is the threshold for a drought season vs. a wet season with $s_S < 1$ indicating drought and $s_S > 1$ indicating wet.

Extremity from temperature:

$$\mathcal{E}_{\text{temp}} = \frac{|s_T|}{5} \quad (38)$$

indicating that $\pm 5^\circ\text{C}$ is the threshold for extreme/not extreme temperature.

Extremity from a drought event:

$$\mathcal{E}_{\text{drought}} = \sum_{(k_0, \kappa, \iota) \in \mathcal{D}} \frac{\kappa}{500} \iota \quad (39)$$

indicating that 500 hours (21 days) constitutes the threshold for long vs. short drought.

Extremity from a heat wave or cold snap event:

$$\mathcal{E}_{\text{heat}} = \sum_{(k_0, \kappa, \iota) \in \mathcal{H}} \frac{\kappa}{200} \frac{\iota}{5} \quad (40)$$

$$\mathcal{E}_{\text{cold}} = \sum_{(k_0, \kappa, \iota) \in \mathcal{C}} \frac{\kappa}{200} \frac{\iota}{5} \quad (41)$$

indicating that a long heat wave or cold snap is considered to be > 500 hours and temperatures are considered to be extreme if 5°C higher or lower than typical.

The aggregate extremity score is then

$$\mathcal{E} = \mathcal{E}_{\text{precip}} + \mathcal{E}_{\text{temp}} + \mathcal{E}_{\text{drought}} + \mathcal{E}_{\text{heat}} + \mathcal{E}_{\text{cold}} \quad (42)$$

4 Model predictive control

4.1 Constrained finite-time optimal control

At each decision epoch, model predictive control (MPC) solves a constrained finite-time optimal control (CFTOC) problem over a planning horizon of K_d days. Discrete-time optimal control is concerned with choosing an optimal input sequence over the horizon K_d

$$\mathcal{U}_{0 \rightarrow K_d} = \{u[k]\} \quad \text{for } k = 0, \dots, K_d - 1 \quad (43)$$

with respect to some objective function over a finite or infinite time horizon in order to apply it to a system with a given initial state $x[0]$. The objective function is often defined as a sum of stage costs $q(x[k], u[k])$ and when the horizon has finite length, a terminal cost $p(x[K_d])$. That is

$$J_{0 \rightarrow K_d}(x[0], \mathcal{U}_{0 \rightarrow K_d}) = p(x[K_d]) + \sum_{n=0}^{K_d-1} q(x[n], u[n]) \quad (44)$$

where the states $\mathcal{X}_{0 \rightarrow K_d} = \{x[k]\} \quad \text{for } k = 0, \dots, K_d - 1$ must satisfy the initial condition and system dynamics

$$\begin{cases} x[0] = x_0 \\ x[k+1] = g(x[k], u[k]) \quad \text{for } k = 0, \dots, K_d - 1 \end{cases} \quad (45)$$

and there may be other state or input constraints formulated as inequalities

$$h(x[k], u[k]) \leq 0 \quad \text{for } k = 0, \dots, K_d - 1 \quad (46)$$

In the finite horizon case, there may also be a terminal constraint requiring the final state to lie in some terminal set $x[K] \in \mathcal{X}_{\text{final}}$.

In our specific case, we construct the problem as a minimization

$$\begin{aligned} J_{0 \rightarrow K_d}^*(x[0]) &= \min_{\mathcal{U}_{0 \rightarrow K_d}} J_{0 \rightarrow K_d}(x[0], \mathcal{U}_{0 \rightarrow K_d}) \quad \text{s.t.} \\ &\begin{cases} x[0] = x_0 \\ x[k+1] = g(x[k], u[k]) \quad \text{for } k = 0, \dots, K_d - 1 \\ x \in \mathbb{R}^+ \\ u \in \mathcal{U} \end{cases} \end{aligned} \quad (47)$$

where the stage cost penalizes input usage and nutrient anomalies:

$$q(x[k], u[k]) = \omega_w \left(\frac{u_w[k]}{u_{w,\text{typ}}} \right)^2 + \omega_f \left(\frac{u_f[k]}{u_{f,\text{typ}}} \right)^2 + \omega_{\Delta w} (\Delta_w[k])^2 + \omega_{\Delta f} (\Delta_f[k])^2 \quad (48)$$

Here ω_w and ω_f are weights on normalized irrigation and fertilizer inputs, $u_{w,\text{typ}}$ and $u_{f,\text{typ}}$ are typical application rates, and $\omega_{\Delta w}$ and $\omega_{\Delta f}$ penalize the cumulative nutrient anomalies Δ_w and Δ_f defined in (5). The terminal cost rewards crop development:

$$p(x[K_d]) = -\omega_h \frac{x_h[K_d]}{k_h} - \omega_A \frac{x_A[K_d]}{k_A} - \omega_P \frac{x_P[K_d]}{k_P} \quad (49)$$

where ω_h , ω_A , and ω_P weight the normalized final height, leaf area, and fruit biomass, respectively. There is no terminal set constraint because we want the plant to grow as much as possible. The terms in the stage cost have been squared in order to encourage sparsity in actuation, more similar to what a farmer might actually implement.

4.2 Solution method

The CFTOC problem is formulated in Pyomo [10] and solved using the IPOPT interior-point nonlinear optimizer [11] with the MUMPS linear solver. The nonlinearity arises from the logistic dynamics, FIR convolution, EMA filtering, and exponential nutrient factor computation. We use an adaptive barrier parameter strategy for robust convergence.

4.3 Receding-horizon algorithm

MPC implements the CFTOC in a receding-horizon fashion, re-optimizing daily based on updated state and weather observations. Let k index the decision day, and let $u[k] = (u_w[k], u_f[k])$ denote the daily irrigation and fertilizer rates. Let $\hat{d}_S, \hat{d}_T, \hat{d}_R$ denote forecast weather and d_S, d_T, d_R denote actual observed weather (precipitation, temperature, radiation).

Algorithm 1 presents the MPC procedure. At each decision day k :

1. Observe current plant state $x[k]$ and obtain K_d -day weather forecast $\{(\hat{d}_S, \hat{d}_T, \hat{d}_R)_{k+i}\}_{i=0}^{K_d-1}$.
2. Solve the CFTOC problem (47) to obtain optimal control sequence $\{u^*[k+j]\}_{j=0}^{K_d-1}$.
3. Apply only the first control $u^*[k] = (u_w[k], u_f[k])$ as constant rates over day k .
4. Simulate hourly plant dynamics over the day using actual (not forecast) weather.
5. Advance to day $k + 1$ and repeat.

Algorithm 1 Model Predictive Control for Irrigation and Fertilization

```

1: Input: Initial state  $x[0]$ , horizon  $K_d$ , season length  $K$  days, weather data
2: Output: Control history  $\{u[k]\}_{k=0}^{K-1}$ , final state  $x[K]$ 
3:
4: Initialize FIR kernel buffers, EMA state variables
5: for  $k = 0$  to  $K - 1$  do
6:   Aggregate hourly weather forecast into daily averages for days  $k, \dots, k + K_d - 1$ 
7:   Solve CFTOC( $x[k], \{(\hat{d}_S, \hat{d}_T, \hat{d}_R)_{k+i}\}_{i=0}^{K_d-1}\} \rightarrow \{u^*[k+i]\}_{i=0}^{K_d-1}$ 
8:   Extract first control:  $(u_w[k], u_f[k]) \leftarrow u^*[k]$ 
9:   for  $t = 0$  to  $23$  do                                 $\triangleright$  Hourly simulation within day  $k$ 
10:    Apply  $(u_w[k], u_f[k])$  with actual weather  $(d_{S,24k+t}, d_{T,24k+t}, d_{R,24k+t})$ 
11:    Update FIR buffers, EMA states, nutrient factors
12:    Advance plant state using closed-form logistic solution (2)
13:  end for
14:   $x_{k+1} \leftarrow$  current plant state
15: end for
16: return  $\{u[k]\}_{k=0}^{K-1}, x[K]$ 

```

4.4 Feedback properties

The key advantage of MPC over open-loop optimization (such as GA) is its closed-loop nature. By re-solving the optimization problem each day with updated state and weather information, MPC can:

- **Correct for forecast errors:** If yesterday’s weather differed from the forecast, today’s optimization accounts for the actual plant state.
- **Adapt to changing conditions:** If a heat wave arrives unexpectedly, MPC can adjust irrigation to maintain nutrient factors.
- **Exploit updated forecasts:** Longer-range forecasts become more accurate as the event approaches.

This adaptivity comes at computational cost—solving a nonlinear optimization problem each day—but modern solvers handle the problem scale (5 state variables, 2 controls, 9-day horizon) in under one second per solve.

5 Bayesian optimization for MPC parameter tuning

The MPC cost function contains seven tunable weights: $\omega_w, \omega_f, \omega_{\Delta w}, \omega_{\Delta f}, \omega_h, \omega_A, \omega_P$, plus the horizon length H . These parameters significantly affect controller behavior, and their optimal values depend on the weather scenario ensemble. We use Bayesian Optimization (BO) to automatically tune these parameters for robust performance.

5.1 Bayesian optimization overview

Standard Gaussian Process (GP) Bayesian Optimization models the objective function as a GP:

$$f(x) \sim \mathcal{GP}(m(x), g(x, x')) \quad (50)$$

where x represents hyperparameter candidates and $f(x)$ is the performance metric. Given observations \mathcal{D}_n , the posterior

$$p(f(x)|\mathcal{D}_n) \sim \mathcal{N}(\mu(x), \sigma_n^2(x)) \quad (51)$$

provides mean and uncertainty estimates that guide acquisition. The next sample is chosen by maximizing an acquisition function:

$$x_{n+1} = \arg \max_x \mathbb{E}(\mu(x), \sigma(x)) \quad (52)$$

balancing exploration (high uncertainty) against exploitation (high predicted value).

Tree-structured Parzen Estimation (TPE) takes an alternative approach: rather than modeling $p(y|x)$ directly, TPE models the inverse $p(x|y)$ using two density functions. Observations are partitioned by a quantile threshold γ (typically 0.1–0.25) into “good” and “bad” sets, with corresponding densities $l(x) = p(x|y \leq y^-)$ and $g(x) = p(x|y > y^-)$, where y^- satisfies

$$P(y \leq y^-) = \gamma, \quad \gamma \in (0, 1) \quad (53)$$

To derive the TPE acquisition function, we begin with expected improvement for minimization:

$$\mathbb{E}[I(x)] = \int_{-\infty}^{y^-} (y^- - y) p(y|x) dy \quad (54)$$

Applying Bayes’ rule $p(y|x) = p(x|y)p(y)/p(x)$:

$$\mathbb{E}[I(x)] = \int_{-\infty}^{y^-} (y^- - y) \frac{p(x|y)p(y)}{p(x)} dy \quad (55)$$

Under the TPE assumption that $p(x|y) \approx l(x)$ for $y \leq y^-$:

$$\mathbb{E}[I(x)] = \frac{l(x)}{p(x)} \int_{-\infty}^{y^-} (y^- - y) p(y) dy \quad (56)$$

Since the integral is constant with respect to x :

$$\mathbb{E}[(I(x))] \propto \frac{l(x)}{p(x)} \quad (57)$$

Expanding $p(x)$ via the law of total probability:

$$p(x) = \gamma l(x) + (1 - \gamma)g(x) \quad (58)$$

yields:

$$\mathbb{E}[I(x)] \propto \frac{l(x)}{\gamma l(x) + (1 - \gamma)g(x)} \quad (59)$$

For fixed γ , maximizing expected improvement is equivalent to maximizing $l(x)/g(x)$, which serves as the TPE acquisition function.

TPE offers computational advantages over GP-based methods and handles mixed parameter spaces (continuous, discrete, categorical) naturally. These properties make TPE well-suited for MPC parameter tuning, where the objective landscape may contain discontinuities from solver failures and the search space includes both continuous weights and integer horizon length.

5.2 Kernel density estimation

TPE approximates the densities $l(x)$ and $g(x)$ using kernel density estimation (KDE). Given samples $\{x_i\}_{i=1}^n$, the kernel density estimator is:

$$\hat{p}(x) = \frac{1}{n} \sum_{i=1}^n g(x, x') \quad (60)$$

with Gaussian kernel $g(x, x') = \mathcal{N}(x|x', h^2)$ and bandwidth h . In one dimension:

$$\hat{p}(x) = \frac{1}{n} \sum_{i=1}^n \frac{1}{\sqrt{2\pi h^2}} \exp \left\{ -\frac{1}{2} \frac{(x - x')^2}{h^2} \right\} \quad (61)$$

For multivariate parameters, TPE assumes independence across dimensions (naive Bayes):

$$l(x) \approx \prod_{j=1}^d l_j(x_j) \quad \text{and} \quad g(x) \approx \prod_{j=1}^d g_j(x_j) \quad (62)$$

Rather than optimizing $l(x)/g(x)$ directly, TPE samples candidates from $l(x)$ and selects the one maximizing $l(x)/g(x)$.

The “tree-structured” aspect of TPE accommodates conditional parameter dependencies—where some parameters are only relevant given certain values of others—by modeling the joint distribution as:

$$p(x) = p(x_1)p(x_2|x_1)p(x_3|x_2)\dots \quad (63)$$

5.3 Search space

Table 1 defines the search space for MPC parameter tuning. Cost weights use log-scale sampling to span multiple orders of magnitude, while value weights and horizon use linear/integer sampling.

Parameter	Lower	Upper	Scale
ω_w (irrigation cost)	0.001	10.0	log
ω_f (fertilizer cost)	0.0001	1.0	log
$\omega_{\Delta w}$ (water anomaly)	0.001	10.0	log
$\omega_{\Delta f}$ (fertilizer anomaly)	0.001	10.0	log
ω_h (height value)	10.0	1000.0	linear
ω_A (leaf area value)	10.0	1000.0	linear
ω_P (fruit biomass value)	100.0	10000.0	linear
H (horizon, days)	3	14	integer

Table 1 Bayesian optimization search space for MPC parameters.

5.4 Robust optimization objective

For robust parameter tuning, we optimize average performance across multiple weather scenarios:

$$\boldsymbol{\theta}^* = \arg \max_{\boldsymbol{\theta}} \frac{1}{|\mathcal{S}|} \sum_{\mathcal{S}_i \in \mathcal{S}} \text{Revenue}(\text{MPC}(\boldsymbol{\theta}, \mathcal{S}_i)) \quad (64)$$

where \mathcal{S} is a representative subset of weather scenarios. This encourages parameters that perform well across diverse conditions rather than overfitting to a single scenario.

5.5 TPE algorithm

Algorithm 2 presents the TPE-based parameter tuning procedure. The objective function averages MPC performance across multiple weather scenarios, encouraging parameters that perform well across diverse conditions rather than overfitting to a single scenario.

Algorithm 2 Bayesian Optimization for MPC Parameter Tuning

```

1: Input: Search space  $\Theta$  (Table 1), weather scenarios  $\mathcal{S}$ , budget  $N$ , startup trials  $N_0$ 
2: Output: Optimal parameters  $\boldsymbol{\theta}^*$ 
3:
4: Initialize TPE surrogate model
5: for  $n = 1$  to  $N$  do
6:   if  $n \leq N_0$  then
7:      $\boldsymbol{\theta}_n \leftarrow$  sample uniformly from  $\Theta$ 
8:   else
9:      $\boldsymbol{\theta}_n \leftarrow \arg \max_{\boldsymbol{\theta}} \text{EI}(\boldsymbol{\theta})$  using TPE
10:  end if
11:
12:   $r_n \leftarrow 0$ 
13:  for each scenario  $\mathcal{S}_i \in \mathcal{S}$  do
14:    Run MPC with parameters  $\boldsymbol{\theta}_n$  on scenario  $\mathcal{S}_i$ 
15:     $r_n \leftarrow r_n + \text{Revenue}_i / |\mathcal{S}|$ 
16:  end for
17:  Update TPE model with observation  $(\boldsymbol{\theta}_n, r_n)$ 
18: end for
19:
20:  $\boldsymbol{\theta}^* \leftarrow \arg \max_n r_n$ 
21: return  $\boldsymbol{\theta}^*$ 

```

We use $N = 100$ trials with $N_0 = 20$ random startup trials before engaging the TPE sampler. For robust optimization, we use a representative subset of 5 scenarios spanning the extremity range.

6 Case study: corn in iowa

We demonstrate the framework using corn, the most widely planted crop in the United States with over 90 million acres harvested annually [12]. The case study uses historical weather data from Fairfax, Iowa (41.76°N , 91.87°W), a representative location in the Corn Belt (USDA climate zones 4b–5b).

6.1 Scenario configuration

The simulation covers a typical growing season from late April to early October (approximately 2900 hours). Environmental inputs are:

- **Temperature and radiation:** Hourly data from NSRDB for Fairfax, IA. Mean temperature is 22.8°C ; mean solar radiation is 580 W/m^2 .
- **Precipitation:** Daily data from NOAA, interpolated to hourly resolution.
- **Typical nutrient expectations:** Based on agronomic recommendations [13], the model expects 28 inches of water and 355 lbs of NPK fertilizer over the season ($w_{\text{typ}} \approx 0.01 \text{ in/hr}$, $f_{\text{typ}} \approx 0.12 \text{ lb/hr}$).

6.2 Three strategies for comparison

We compare three irrigation and fertilization strategies representing different approaches to resource management:

Farmer Baseline. Standard agronomic best practices based on published recommendations [14, 15]: weekly irrigation at 1 inch per application, and monthly fertilization at 90 lbs per application. This represents what a well-informed farmer might implement without optimization.

Fixed GA. A strategy optimized via genetic algorithm [6] for drought conditions (50% of normal precipitation). The GA searches over four parameters—irrigation frequency, irrigation amount, fertilizer frequency, and fertilizer amount—to maximize net revenue. The optimal strategy applies irrigation every 52 days at 5.0 inches per application, and fertilizer every 33 days at 77 lbs per application. This represents the best fixed strategy when drought is anticipated.

Adaptive MPC. Model Predictive Control that re-optimizes daily based on observed weather and current plant state. Unlike the fixed strategies, MPC adjusts resource allocation throughout the growing season in response to actual conditions.

Table 2 summarizes the control parameters for each strategy.

Strategy	Irrig. Freq. (days)	Irrig. Amt. (in)	Fert. Freq. (days)	Fert. Amt. (lbs)
Farmer Baseline	7	1.0	30	90
Fixed GA	52	5.0	33	77
Adaptive MPC	Daily re-opt.	Variable	Daily re-opt.	Variable

Table 2 Control parameters for the three strategies compared in this study.

6.3 MPC configuration

The MPC controller uses a 9-day planning horizon ($K_d = 9$) with daily re-optimization. Control bounds are set to $u_w \in [0, 0.7]$ inches/hour and $u_f \in [0, 12]$ lbs/hour, reflecting practical application rate limits.

MPC weight parameters were tuned using Bayesian optimization (100 trials) to maximize robust performance across 5 representative weather scenarios. The optimal parameters are:

- Input costs: $\omega_w = 0.177 \text{ \$/inch}$, $\omega_f = 0.002 \text{ \$/lb}$
- Anomaly penalties: $\omega_{\Delta w} = 2.94$, $\omega_{\Delta f} = 1.21$
- Value weights: $\omega_h = 590.8 \text{ \$/m}$, $\omega_A = 491.0 \text{ \$/m}^2$, $\omega_P = 1203.3 \text{ \$/kg}$

Note that these weights differ from the economic weights used in the GA cost function; they are tuned to optimize MPC behavior rather than represent true economic values.

6.4 Weather scenario suite

We evaluate both GA and MPC across 21 stochastic weather scenarios generated from the baseline historical data. Table 3 summarizes the scenario categories.

Category	Count	Extremity Range
Normal	5	0.03–0.18
Moderate	5	0.35–0.90
Drought	4	1.20–2.45
Wet/Cool	2	0.95–1.10
Heat Stress	2	2.10–3.50
Extreme	2	5.60–8.38

Table 3 Weather scenario categories with extremity index ranges.

6.5 Results

Table 4 presents summary statistics for all three strategies across the 21 weather scenarios. Both optimization-based methods substantially outperform farmer baseline practices, with the Fixed GA achieving the highest mean revenue and MPC achieving the lowest variance.

Strategy	Mean (\$/acre)	Std Dev	CV (%)	Min	Max
Farmer Baseline	626	135	21.6	385	853
Fixed GA	796	132	16.6	550	997
Adaptive MPC	750	115	15.4	445	886

Table 4 Summary statistics for the three strategies across 21 weather scenarios. CV = coefficient of variation (standard deviation / mean).

Both the Fixed GA and MPC outperform farmer baseline in all scenarios, with mean advantages of \$170/acre and \$123/acre, respectively. When comparing GA to MPC directly, MPC wins in 12 of 21 scenarios, while GA wins in the remaining 9. The key insight is *which* scenarios favor each strategy.

Table 5 presents results for representative scenarios spanning the extremity range. MPC outperforms GA in normal and wet conditions, where the GA’s drought-optimized strategy applies more resources than necessary. Conversely, GA outperforms MPC in drought scenarios, where its optimization assumptions match actual conditions.

Scenario	Extremity	Farmer	Fixed GA	MPC	MPC-GA
normal_1 (baseline)	0.00	587	784	848	+64
moderate_wet	0.70	453	629	716	+87
moderate_dry	0.80	721	913	796	-116
wet_year	1.10	385	551	633	+82
mild_drought	1.30	853	997	717	-280
summer_drought	1.70	752	944	746	-197
heat_stress	1.70	669	855	795	-60
extreme_drought_heat	4.97	768	836	518	-317
worst_case	8.38	659	734	445	-289

Table 5 Revenue (\$/acre) for representative scenarios. MPC outperforms GA in normal/wet conditions; GA outperforms MPC in drought conditions.

Figure 1 visualizes revenue across all 21 scenarios, sorted by increasing extremity index. The divergence between strategies is evident: MPC (green) consistently outperforms in the left portion of the plot (normal conditions), while Fixed GA (orange) dominates in the right portion (drought and extreme conditions).

6.6 Performance by weather type

To better understand when each strategy excels, we categorize scenarios by their dominant characteristic and compute mean revenue within each category (Table 6).

The pattern is clear: MPC outperforms the Fixed GA by \$65/acre on average in normal conditions and by \$91/acre in wet/cool conditions. However, the Fixed GA outperforms MPC by \$258/acre in drought scenarios and by \$303/acre in the most extreme combined scenarios. This divergence reflects the fundamental difference in approach: the GA was optimized for drought and performs best when those

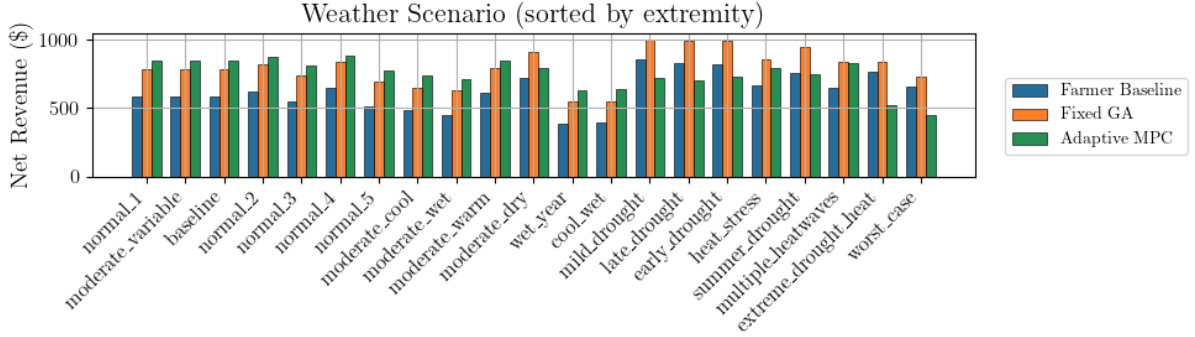


Fig. 1 Revenue comparison across all 21 weather scenarios, sorted by extremity index. Farmer Baseline (blue), Fixed GA (orange), and Adaptive MPC (green). Both optimization-based methods outperform the baseline in all scenarios. MPC excels in normal/wet conditions (left), while Fixed GA excels in drought conditions (right).

Weather Type	n	Farmer	Fixed GA	MPC
Normal/Baseline	7	571	764	829
Wet/Cool	4	419	590	681
Drought	4	814	981	723
Heat Stress	4	685	851	762
Extreme Combined	2	713	785	482

Table 6 Mean revenue (\$/acre) by weather category.
MPC excels in normal and wet conditions; GA excels in drought conditions.

assumptions hold, while MPC adapts to observed conditions but cannot anticipate future drought stress as effectively. Figure 2 illustrates this pattern visually.

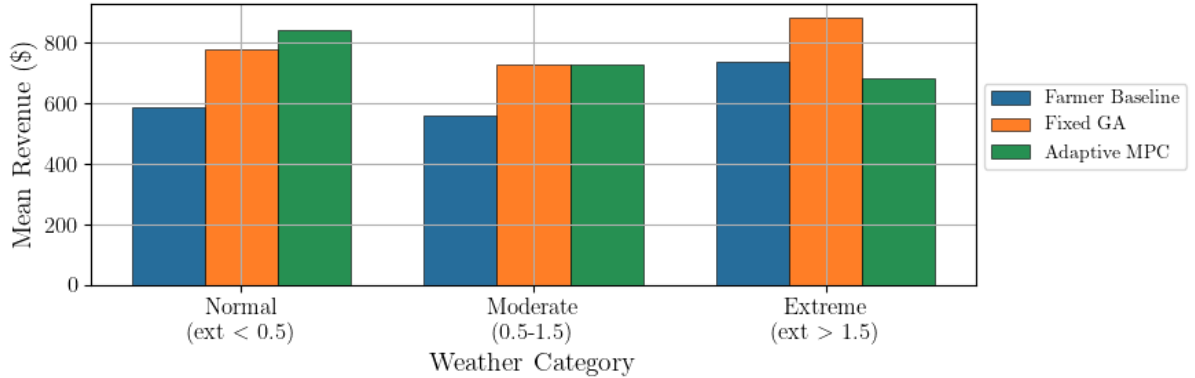


Fig. 2 Mean revenue by weather category. MPC (green) outperforms Fixed GA (orange) in normal and moderate conditions, while Fixed GA dominates in drought and extreme scenarios. Both optimization methods substantially outperform Farmer Baseline (blue) across all categories.

6.7 Variance and risk analysis

The coefficient of variation (CV), defined as the ratio of standard deviation to mean, provides a normalized measure of consistency:

$$CV = \frac{\sigma}{\mu} \times 100\% \quad (65)$$

As shown in Table 4, MPC achieves the lowest CV (15.4%) compared to the Fixed GA (16.6%) and Farmer Baseline (21.6%). This indicates that MPC delivers the most consistent relative performance across the diverse weather scenarios, even though its mean revenue is lower than the Fixed GA.

The risk-return tradeoff becomes apparent when examining the full distribution. The Fixed GA achieves the highest maximum revenue (\$997/acre in mild drought) but also experiences larger swings: its revenue ranges from \$550 to \$997, a spread of \$447. MPC's range is tighter at \$441 (\$445 to \$886), despite having a lower floor.

For risk-averse decision-makers, this tradeoff is significant. Consider a farmer who must meet fixed costs of \$600/acre. The Fixed GA falls below this threshold in 2 scenarios (wet_year and cool_wet), while MPC falls below in 3 scenarios (the same two plus worst_case). However, when conditions are uncertain—when the farmer cannot predict whether drought or flooding is more likely—MPC's lower variance may be preferable because it reduces exposure to large deviations from expected performance.

Figure 3 shows the revenue distribution for each strategy as a box plot. The Fixed GA has the highest median and mean (red diamond), but also exhibits greater spread. MPC's distribution is more compact, reflecting its consistent performance across diverse conditions.

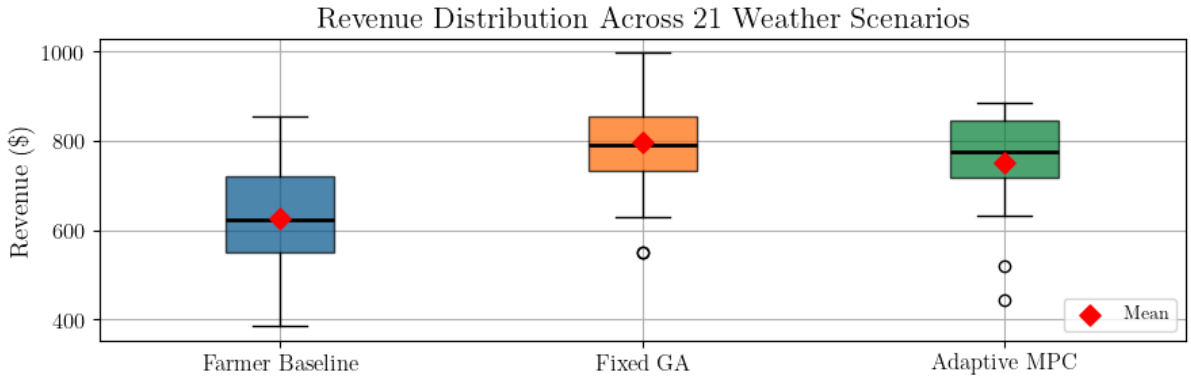


Fig. 3 Revenue distribution across 21 weather scenarios. Box plots show median (black line), interquartile range (box), and full range (whiskers). Red diamonds indicate means. MPC exhibits the most compact distribution despite a lower mean, indicating more consistent performance.

Figure 4 directly compares the coefficient of variation for each strategy. MPC achieves a 7% reduction in relative variability compared to the Fixed GA (15.4% vs 16.6%), and a 29% reduction compared to Farmer Baseline (15.4% vs 21.6%). This consistency is a key advantage for operations that prioritize predictable outcomes over maximum expected returns.

6.8 Resource usage patterns

MPC's adaptive nature is evident in its resource usage across scenarios. While GA applies the same total irrigation regardless of conditions, MPC irrigation varies from 3.9 inches (wettest scenario) to 6.3 inches (driest scenario). This adaptation allows MPC to conserve water when natural precipitation is sufficient while providing additional irrigation when stress threatens crop development.

7 Discussion

7.1 Interpretation of results

Our results reveal that the choice between fixed and adaptive strategies depends critically on the nature of weather uncertainty. This finding has important practical implications.

When fixed optimization excels. If climate trends are predictable—for example, if a region is experiencing increasing drought frequency due to climate change—then optimizing a fixed strategy for those expected conditions can be highly effective. In our study, the GA-optimized strategy achieved \$997/acre under mild drought, the highest revenue of any strategy in any scenario. For farmers in regions where drought is the dominant concern, such a strategy may be optimal.

When adaptive control excels. If weather patterns are uncertain or variable—if both drought and flooding are plausible within the planning horizon—then MPC provides valuable insurance. MPC achieved \$633–716/acre in wet conditions, compared to only \$550–630 for the Fixed GA. The GA's drought-optimized parameters (infrequent, heavy irrigation) are poorly suited to wet conditions, where lighter, more frequent applications would be preferable.

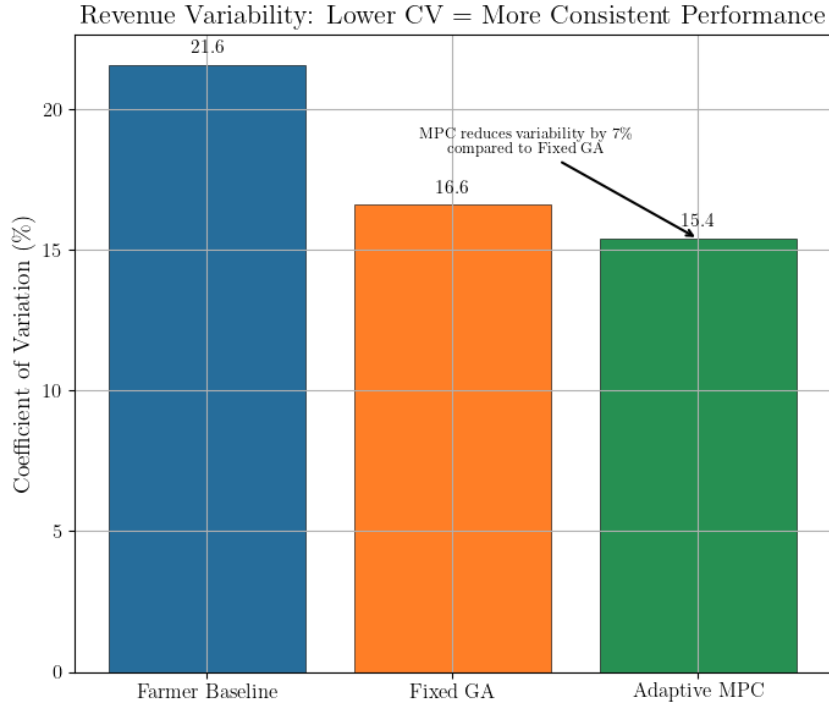


Fig. 4 Coefficient of variation (CV) comparison. Lower CV indicates more consistent relative performance. MPC achieves the lowest CV (15.4%), followed by Fixed GA (16.6%) and Farmer Baseline (21.6%).

The value of adaptability. MPC’s adaptive behavior is evident in its resource usage patterns. While the Fixed GA applies the same total irrigation in every scenario, MPC varies its irrigation from approximately 3.9 inches in the wettest scenario to 6.3 inches in the driest. This responsiveness allows MPC to conserve resources when conditions are favorable and apply additional inputs when stress threatens crop development.

Risk-return tradeoff. The comparison reveals a classic risk-return tradeoff. The Fixed GA maximizes expected revenue but with higher variance; MPC achieves lower expected revenue but with the most consistent performance (lowest CV). For operations with significant fixed costs or limited financial reserves, MPC’s consistency may be preferable despite the lower mean. For operations that can absorb year-to-year variability, the Fixed GA’s higher expected return may be more attractive.

7.2 Computational considerations

Each CFTOC solve requires approximately 0.5–1.0 seconds on a modern workstation using IPOPT. Over a 121-day growing season with daily re-optimization, total computation time is approximately 1–2 minutes.

The Bayesian optimization for parameter tuning requires 100 trials, each involving multiple full-season MPC simulations. Total tuning time is approximately 2–4 hours, but this is a one-time offline computation. Once parameters are tuned, MPC operates with minimal computational burden.

7.3 Limitations and extensions

Several limitations suggest directions for future work:

Perfect forecast assumption. Our MPC formulation assumes perfect weather forecasts over the planning horizon. In practice, forecast accuracy degrades with lead time. Incorporating forecast uncertainty through stochastic MPC or robust optimization would improve real-world applicability.

Single-point model. The crop model represents a single plant without spatial heterogeneity. Field-scale implementation would require accounting for spatial variation in soil properties, drainage, and microclimate.

Simplified economics. Our cost function uses constant economic weights. In practice, crop prices fluctuate seasonally, and input costs may have nonlinear components (e.g., volume discounts, capacity constraints).

Daily control resolution. We optimize daily-average irrigation and fertilizer rates. Finer temporal resolution (e.g., hourly) could capture within-day dynamics but would substantially increase computational cost.

Additional control variables. The current formulation considers only irrigation and fertilizer. Other controllable factors—such as planting date, crop variety selection, or deficit irrigation strategies—could be incorporated into the optimization framework.

8 Conclusion

This paper presented a comparative study of fixed versus adaptive irrigation and fertilization strategies under weather uncertainty. We developed an MPC framework with Bayesian-optimized parameters and evaluated it against both farmer baseline practices and a GA-optimized fixed strategy across 21 stochastic weather scenarios.

Our key findings are:

1. Both optimization-based methods (GA and MPC) substantially outperform farmer baseline practices, with mean advantages of \$170/acre and \$123/acre, respectively.
2. The Fixed GA achieves the highest mean revenue (\$796/acre) but with higher variance, while MPC achieves lower mean revenue (\$750/acre) but with the lowest coefficient of variation (15.4% vs 16.6%).
3. MPC outperforms the Fixed GA in 12 of 21 scenarios—primarily in normal and wet conditions—while the Fixed GA excels in drought scenarios for which it was optimized.
4. The choice between strategies involves a risk-return tradeoff: fixed optimization maximizes expected returns when conditions match assumptions; adaptive control provides consistency when weather is uncertain.

These findings have practical implications for agricultural decision-making. In regions with predictable climate trends (e.g., increasing drought frequency), optimizing a fixed strategy for those expected conditions can be highly effective. In regions with variable or uncertain weather patterns, adaptive MPC provides valuable risk reduction through consistent performance.

The computational overhead of MPC is modest—daily optimization solves complete in under one second—making real-time implementation feasible. The framework is generalizable to other crops through re-parameterization of the underlying growth model.

Future work will incorporate forecast uncertainty through stochastic MPC, extend to field-scale spatial heterogeneity, and validate against field trial data. Additionally, exploring hybrid strategies that combine fixed optimization with adaptive adjustments may capture benefits of both approaches.

Acknowledgements. This work has been partially supported by the UC Berkeley College of Engineering and the USDA AI Institute for Next Generation Food Systems (AIFS), USDA award number 2020-67021-32855.

Declarations

Competing Interests The authors declare that they have no known competing financial interests or personal relationships that could have appeared to influence the work reported in this paper.

Code availability The source code used for this study is archived on Zenodo at <https://doi.org/10.5281/zenodo.18204023>.

Declaration of generative AI and AI-assisted technologies in the manuscript preparation process During the preparation of this work the authors used ChatGPT and Claude Code in order to generate some portions of the code base, though no underlying theory, and refine the original drafts of the paper. After using this tool/service, the authors reviewed and edited the content as needed and take full responsibility for the content of the published article.

References

- [1] IPCC: Climate change 2021: The physical science basis. contribution of working group i to the sixth assessment report of the intergovernmental panel on climate change. Technical report, Cambridge University Press (2021). <https://doi.org/10.1017/9781009157896>

- [2] Zohdi, T.I.: A machine-learning enabled digital-twin framework for next generation precision agriculture and forestry. *Computer Methods in Applied Mechanics and Engineering* **428**, 117250 (2024) <https://doi.org/10.1016/j.cma.2024.117250>
- [3] Mengi, E., Samara, O.A., Zohdi, T.I.: Crop-driven optimization of agrivoltaics using a digital-replica framework. *Smart Agricultural Technology* **4**, 100150 (2023) <https://doi.org/10.1016/j.atech.2022.100150>
- [4] Betancourt, J.O., Li, I., Mengi, E., Corrales, L., Zohdi, T.I.: A computational framework for precise aerial agricultural spray delivery processes. *Archives of Computational Methods in Engineering* (2024) <https://doi.org/10.1007/s11831-024-10106-6>
- [5] Tagkopoulos, I., Brown, S.F., Liu, X., Zhao, Q., Zohdi, T.I., Earles, J.M., Nitin, N., Runcie, D.E., Lemay, D.G., Smith, A.D., Ronald, P.C., Feng, H., Youtsey, G.D.: Special report: AI institute for next generation food systems (AIFS). *Computers and Electronics in Agriculture* **196**, 106819 (2022) <https://doi.org/10.1016/j.compag.2022.106819>
- [6] Becker, C.J., Zohdi, T.I.: Optimizing irrigation and fertilizer strategy using a crop growth model with delayed nutrient absorption dynamics. *Computers and Electronics in Agriculture* (2025). Under review
- [7] Rawlings, J.B., Mayne, D.Q., Diehl, M.: *Model Predictive Control: Theory, Computation, and Design*, 2nd edn. Nob Hill Publishing, ??? (2017)
- [8] Shahriari, B., Swersky, K., Wang, Z., Adams, R.P., Freitas, N.: Taking the human out of the loop: A review of Bayesian optimization. *Proceedings of the IEEE* **104**(1), 148–175 (2016) <https://doi.org/10.1109/JPROC.2015.2494218>
- [9] Bergstra, J., Bardenet, R., Bengio, Y., Kégl, B.: Algorithms for hyper-parameter optimization. In: *Advances in Neural Information Processing Systems*, vol. 24, pp. 2546–2554 (2011). <https://doi.org/10.5555/2986459.2986743>
- [10] Bynum, M.L., Hackebeil, G.A., Hart, W.E., Laird, C.D., Nicholson, B.L., Sirola, J.D., Watson, J.-P., Woodruff, D.L.: *Pyomo—Optimization Modeling in Python*, 3rd edn. Springer, ??? (2021). <https://doi.org/10.1007/978-3-030-68928-5>
- [11] Wächter, A., Biegler, L.T.: On the implementation of an interior-point filter line-search algorithm for large-scale nonlinear programming. *Mathematical Programming* **106**(1), 25–57 (2006) <https://doi.org/10.1007/s10107-004-0559-y>
- [12] USDA Farm Service Agency: Acreage Data. <https://www.fsa.usda.gov/news-room/efoia/electronic-reading-room/frequently-requested-information/crop-acreage-data>. Accessed: 2024 (2024)
- [13] Sawyer, J.E., Mallarino, A.P.: Nutrient management for corn following corn. Technical Report PM 2088, Iowa State University Extension (2017)
- [14] Kranz, W.L., Irmak, S., Donk, S.J., Yonts, C.D., Martin, D.L.: Irrigation management for corn. NebGuide (G1850) (2008)
- [15] Davies, B., Coulter, J.A., Pagliari, P.H.: Timing and rate of nitrogen fertilization influence maize yield and nitrogen use efficiency. *PLoS ONE* **15**(5), 0233674 (2020) <https://doi.org/10.1371/journal.pone.0233674>